Vol 1 | Issue 6|2020

Ophthal Focus

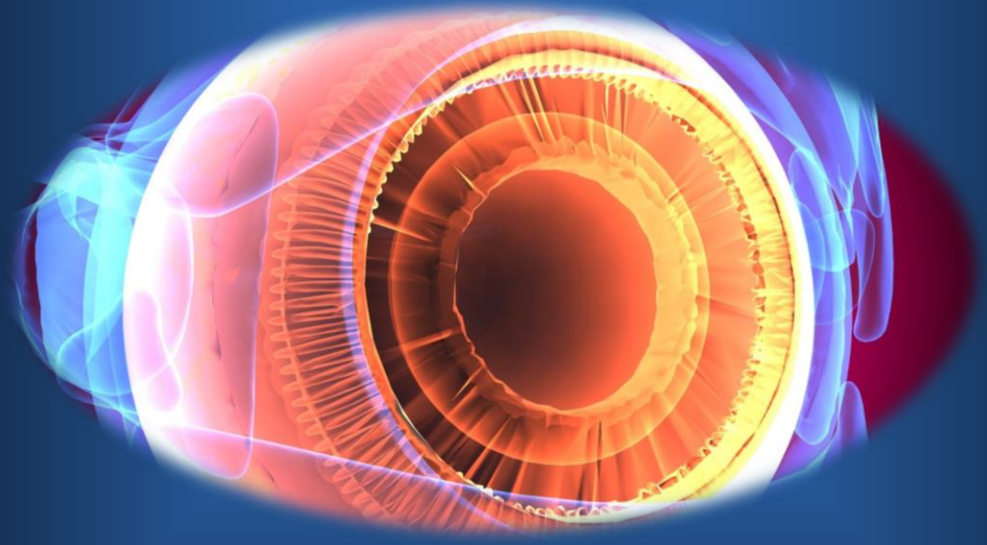

Dear Doctor,

Greetings from Micro Labs Limited. We are happy to bring you 'Ophthal Focus' which contains latest and interesting news in the field of Ophthalmology.

This issue contains

- Prevalence of Persistent Corneal Epithelial Defects in Chronic Ocular Graft- Versus-Host Disease
- Clinical and imaging factors associated with the outcomes of tubercular serpiginous like choroiditis
- Abruptly emerging vessels in eyes with myopic patchy chorioretinal atrophy

Should you require any specific article or medical information, please feel free to contact us at medicalservices@microlabs.in
Looking forward to your valuable feedback

Best Regards

Prevalence of Persistent Corneal Epithelial Defects in Chronic Ocular Graft- Versus-Host Disease

The analysis shows that oGVHD patients with diabetes, LSCD, filamentary keratitis, subconjunctival fibrosis and a high NIH score are at higher risk of developing severe corneal disease.

Advancements in the field of allogeneic hematopoietic stem cell transplantation (HSCT) have facilitated the management of various malignant and non-malignant hematologic diseases. As outcomes improve, the frequency of these procedures also continues to increase. Graft versus-host disease (GVHD) is a significant and potentially life-threatening complication of allogeneic HSCT. Following stem cell transplantation, donor-derived T-cells recognize host antigens as foreign, and may subsequently mount a response against host tissues, including ocular tissue. Ocular GVHD (oGVHD) occurs in 40-60% of patients undergoing HSCT and can have a significant negative impact on patient quality of life. This restrospective cohort study was conducted to establish the prevalence, clinical characteristics, and risk factors for persistent corneal epithelial defects (PED) in patients with chronic ocular graft-versus-host disease (oGVHD) and to determine visual outcomes after healing.

A chart review of patients diagnosed with chronic oGVHD was performed between January 2011 and December 2018 and recorded their demographic and clinical characteristics. The data were analyzed to determine prevalence

of PED and multivariate logistic regression was performed to determine the risk factors associated with it.

A total of 405 patients diagnosed with chronic oGVHD with a mean age of 60±13 years; 58% were men. The prevalence of PED was 8.1%; the median time for PED development after hematopoietic stem cell transplantation was approximately 24 months. Median time to PED resolution was 4.5 weeks after starting therapy. The mean best-corrected visual acuity declined by two lines post-PED resolution. The prevalence rates of corneal ulcer and perforation were 6.2% and 4.0%, respectively, over eight years. Logistic regression analysis to determine factors associated with PED showed diabetes (p=0.006), limbal stem cell deficiency (LSCD) (p=0.02), filamentary keratitis(p=0.02), subconjunctival fibrosis(p=0.02) and a higher oGVHD NIH core(p=0.01) to be significant risk factors for PED development.

The prevalence rate of PED, corneal ulceration and corneal perforation in chronic oGVHD was found to be 8.1%, 6.2%, and 4%, respectively. The analysis shows that oGVHD patients with diabetes, LSCD, filamentary keratitis, subconjunctival fibrosis and a high NIH score are at higher risk of developing severe corneal disease.

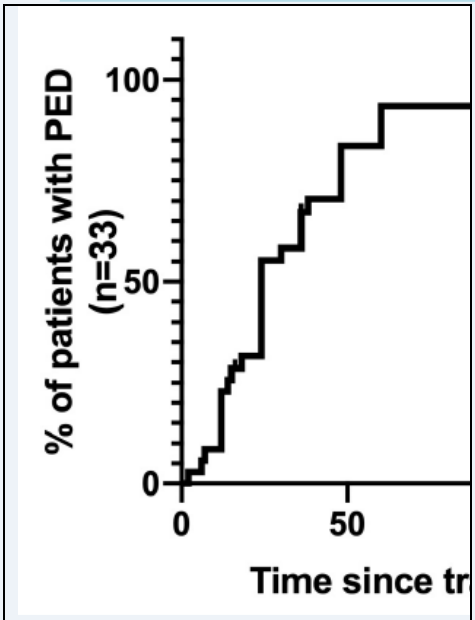

Kaplan Meier analysis of PED presentation in patients with oGVHD disease.

Source: Sinha S et al. American J Ophthal 2020 July. Online ahead of print. doi: https://doi.org/10.1016/j.ajo.2020.05.035.

This study shows that TB SLC lesions that have a higher grade of opacity at baseline may be associated with overall poor response to treatment, greater risk of lesion progression, and paradoxical worsening during the follow-up.

Clinical and imaging factors associated with the outcomes of tubercular serpiginous like choroiditis

Tubercular serpiginous-like choroiditis (TB SLC) is a recurrent inflammation of the choriocapillaris, choroid, and the retinal pigment epithelium seen in patients with evidence of systemic or latent tuberculosis. TB SLC often affects young adults in the working-age group and is characterized by relentless progression with multiple recurrences if specific therapy is not initiated. The

disease is believed to be an autoimmune response to Mycobacterium tuberculosis and is typically managed with systemic corticosteroids and immunosuppression to treat the inflammation along with anti-tubercular treatment (ATT) to reduce disease recurrences. Development of complications such as choriocapillaris atrophy and choroidal neovascularization may occur over the follow-up leading to severe visual loss.

The present study primarily aims to determine whether the anatomical characteristics of active lesions of TB SLC at the time of presentation can predict (a) the development of paradoxical worsening, and (b) progression of the lesions despite standard therapy.

In this retrospective clinical study, Charts and fundus photos of consecutive patients with active TB SLC seen at a single tertiary referral center with 6 months follow-up after initiation of treatment were reviewed. Logistic mixed models were performed to determine the clinical and imaging factors associated with the response to therapy, including the opacity of choroiditis graded according to a three-point scale. This study included 203 eyes of 183 patients with active TB SLC. Poor initial visual acuity (BCVA), foveal and optic disc involvement were associated with poor response to therapy at six months (odds ratio – OR – 4.489, 95%CI: 1.92-10.47; $p<0.001$; OR – 2.892, 95%CI: 1.23-6.81; $p=0.015$; OR – 11.633, 95%CI: 3.17-42.71; $p<0.001$, respectively).

	UNIVARIABLE		MULTIVARIABLE	
Variable	OR (95% CI)	P-value	OR (95% CI)	P-value
Age, per 1-year increase	0.957 (0.927−0.988)	**0.006**	0.959 (0.923-0.997)	**0.034**
Male sex	1.473 (0.777−2.794)	0.24	1.116 (0.511-2.434)	0.78
Right eye	0.673 (0.374−1.211)	0.19		
Baseline BCVA >0.7 LogMAR	4.069 (1.976−8.376)	**<0.001**	2.212 (1.008-4.852)	**0.048**
Opacity grade 2+3 (ref: grade 1)	24.605 (6.685−90.556)	**<0.001**	7.236 (2.003-26.146)	**0.003**
Placoid subtype (ref: multifocal)	1.497 (0.671−3.341)	0.32		
Fovea involved	5.254 (2.821−9.786)	**<0.001**	3.681 (1.71-7.922)	**0.001**
Optic disc involved	9.544 (4.36−20.894)	**<0.001**	5.836 (2.306-14.772)	**<0.001**

Only age, gender, and variables with a p≤0.05 at univariable analysis were included in the multivariable model.

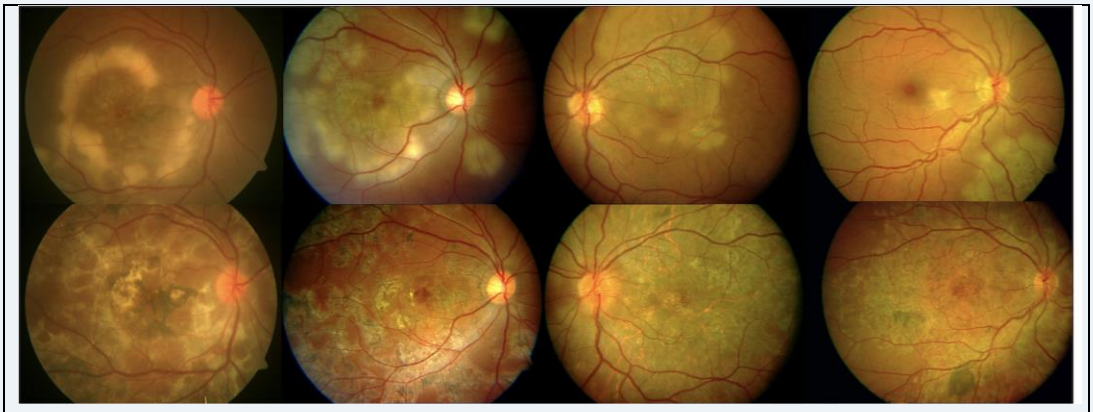

Figure. Eyes showing poor response to therapy of tubercular serpiginous-like choroiditis. (Top row) Baseline fundus photographs illustrate intense yellow-white lesions of active choroiditis. (Bottom row) After 6 months of follow-up, fundus photographs show a significant increase in the final size of the lesions from baseline.

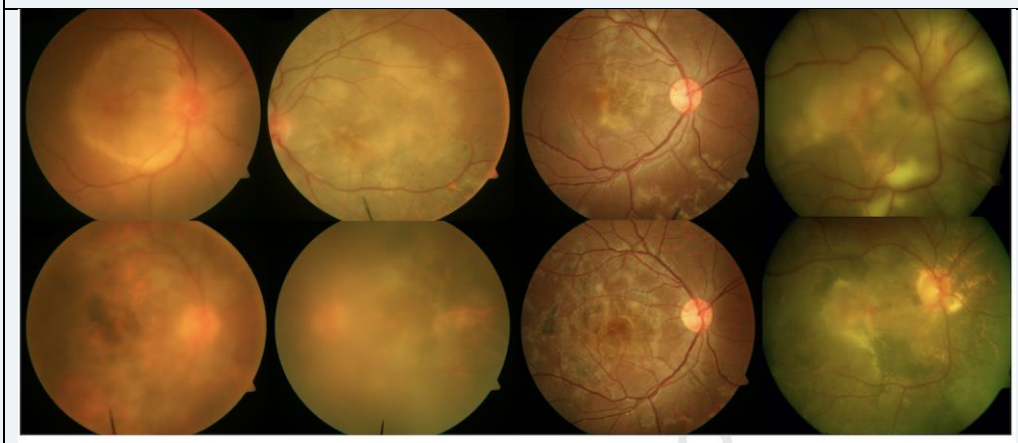

Figure. Eyes showing paradoxical worsening of tubercular serpiginous-like choroiditis.

(Top row) Baseline fundus photographs illustrate intense yellow-white lesions of active choroiditis. (Bottom row) Following initiation of anti-tubercular treatment, fundus photographs show the paradoxical worsening of tubercular serpiginous-like choroiditis.

The high opacity grades (2 and 3) were also associated with poor outcomes and showed the highest OR (9.541; 95%CI: 2.94-30.91; p=0.001). Poor baseline BCVA and high grade of opacity of the lesions were the composite risk factors for paradoxical worsening of TB SLC (OR – 4.489, 95%CI: 1.92-10.47; p=0.001; OR – 9.541, 95%CI: 2.94-30.91; p<0.001, respectively).

AEVs were found in 43.1% of eyes with myopic PA. A slight bowing of the sclera was found around the AEVs in 41 of 69 eyes.

In conclusion, this study shows that TB SLC lesions that have a higher grade of opacity at baseline may be associated with overall poor response to treatment, greater risk of lesion progression, and paradoxical worsening during the follow-up. Other factors such as young age, peripapillary and macular involvement, and placoid phenotype of TB SLC are also risk factors for poor outcomes. In future prospective studies, grading of baseline lesion opacity may be used to predict the biological behavior of the lesions and validate the results of this study, and may serve as a guide to therapeutic interventions.

Source: Agarwal A et al. American J Ophthal 2020 Jul. doi: https://doi.org/10.1016/j.ajo.2020.07.024.

Abruptly emerging vessels in eyes with myopic patchy chorioretinal atrophy

Pathologic myopia (PM) is a major cause of visual impairments especially in the East Asian populations. The cause of the visual impairments is the

development of various macular lesions specific to PM. The META-PM study group2 established a photographic classification of myopic maculopathy which included diffuse chorioretinal atrophy, patchy chorioretinal atrophy, lacquer cracks, myopic chorioretinal neovascularization, and macular atrophy which are predominantly myopic chorioretinal neovascularization-related macular atrophies. Patchy atrophy (PA), another type of myopic maculopathy, is seen ophthalmoscopically as a whitish lesion with well-defined borders. Optical coherence tomographic images show that the entire thickness of the choroid, except for sporadic large vessels, retinal pigment epithelium (RPE), and outer retina is absent in the areas of PA. Thus, the inner retina sits directly on the sclera. Because of the loss of the photoreceptors, an absolute scotoma is present in the visual field corresponding to the patchy atrophic area. The PA rarely involves the central fovea, and thus, the central vision is usually maintained in eyes with PA.

The purpose of this study was to determine the prevalence and characteristics of AEVs within and at the edge of the areas of PA regardless of the presence of focal scleral ectasia. 160 highly myopic eyes of 144 patients between March and November in 2016. Fundus photographs and swept-source optical coherence tomography images were analyzed. Patient mean age was 67.1 ± 10.5 years. Mean axial length was 30.9 ± 2.0 mm^2

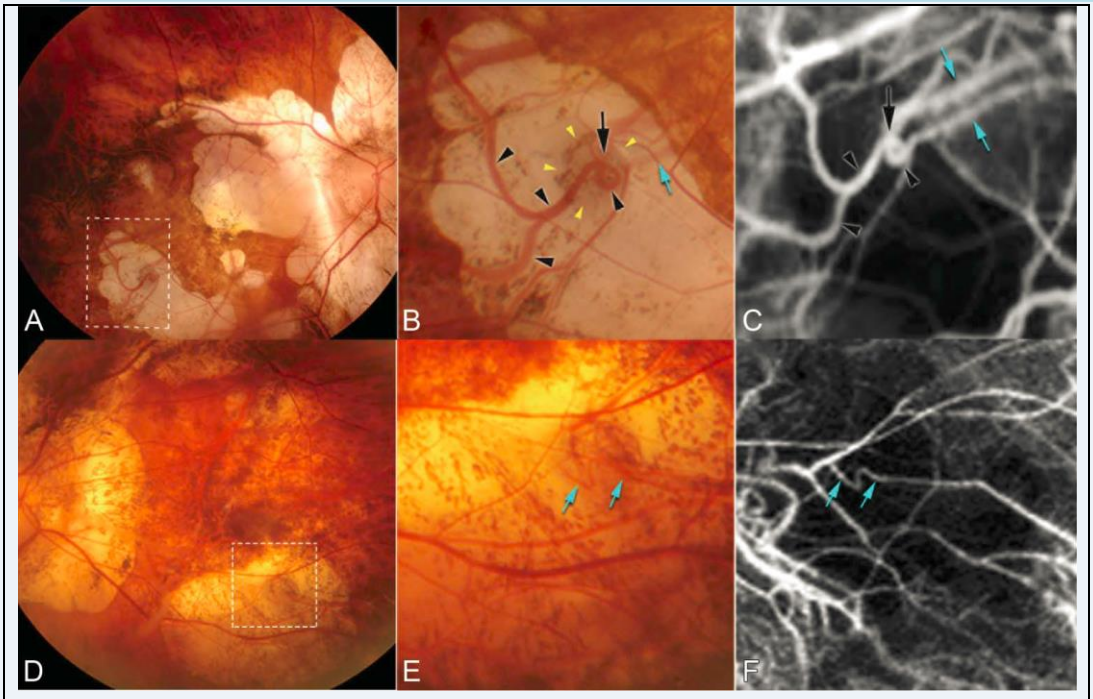

Fig: Origin of AEVs determined by examinations of both fundus photographs and earlyphase ICGA images. A. Right fundus of a 79-year-old woman with an axial length of 32.9 mm shows multiple areas of PA in and around the macular region (The same patient in Figure 1, I– K). B. Magnified image of square area in (A). One large vessel abruptly emerges (black arrow), then takes a curled turn and then courses within the area of PA, and finally continues as a choroidal vessel outside the PA (shown by black arrowheads). There is a slightly darker area (margined by yellow arrowheads) around the emerging site of this vessel. The surrounding area shows a different reflection with blurred border (yellow arrowheads). C. Early phase of ICG angiography shows the course of this emerging vessel (arrowheads). Black arrow shows the same point as image (B) which is the possible site where this vessel appears in the fundus photograph. Two parallel running vessels are seen in the ICG angiogram (blue arrows), and they seem to be continuous with the vessel shown by black arrowheads. Among these two vessels, the lower vessel is vaguely seen in the fundus photograph (blue arrow in B). D. Left fundus of a 65-year-old woman. The axial length of the eye was 31.97 mm. A PA can be seen inferior to the fovea (same patient in Figure 5, G–I). E. Magnified image of the square area in (D). An abrupt appearance of a folded vessel can be seen (blue arrows). F. Early-phase ICGA shows the same vessel as in (E). The vessel is a branch from a SPCA.

The mean size of the 264 PAs was 5.6 ± 8.3 mm^2. Abruptly emerging vessels were detected in 69 (43.1%) eyes and were located within or near PA edge in fundus photographs. Swept source optical coherence tomography showed that the AEVs were continuous with perforating scleral vessels and were observed on the inner surface of the sclera at the site where they appeared in fundus photographs. A slight bowing of sclera around the AEVs was observed in 41 (59%) eyes. Patchy atrophy with AEVs was significantly larger (10.7 ±11.3 mm^2) than PA without AEVs (3.4 ± 5.1 mm^2).

The average size of the patchy atrophic lesions with AEVs was 10.7 mm^2 ± 11.3 mm^2 (range, 0.1–50.8 mm^2) which was significantly larger than the 3.4 mm2 ± 5.1 mm^2 (range: 0.1–37.6 mm^2) of the lesions without AEVs. More specifically, the PA was significantly larger in AEV-present lesions than AEV-absent lesions at the temporal area (P <0.001), superior area (P<0.001), and inferior area (P = 0.001; Table).

Location†	AEV Present Size (Median, mm^2)	AEV Absent Size (Median, mm^2)	*P**
Macular	2.3 ± 3.0 (1.4)	2.5 ± 4.2 (1.4)	>0.999
Superior	11.7 ± 13.9 (7.2)	2.1 ± 3.0 (1.0)	<0.001
Inferior	12.5 ± 12.3 (9.6)	5.0 ± 7.2 (2.2)	0.001
Temporal	12.6 ± 9.8 (11.2)	3.0 ± 2.8 (2.1)	<0.001
Nasal	1.2 ± 1.2 (1.0)	5.6 ± 9.2 (1.0)	0.250
Total	10.7 ± 11.3 (7.5)	3.4 ± 5.1 (1.6)	<0.001

*Mann–Whitney *U* test.

Comparison of Size of PA Between the Eyes With and Without AEVs

In 26 eyes, 12 eyes had fundus photographs available before the formation of the PA. By comparing the long-term fundus changes of the PA, nine eyes were observed with PA primarily at the AEV site (Figure 3).

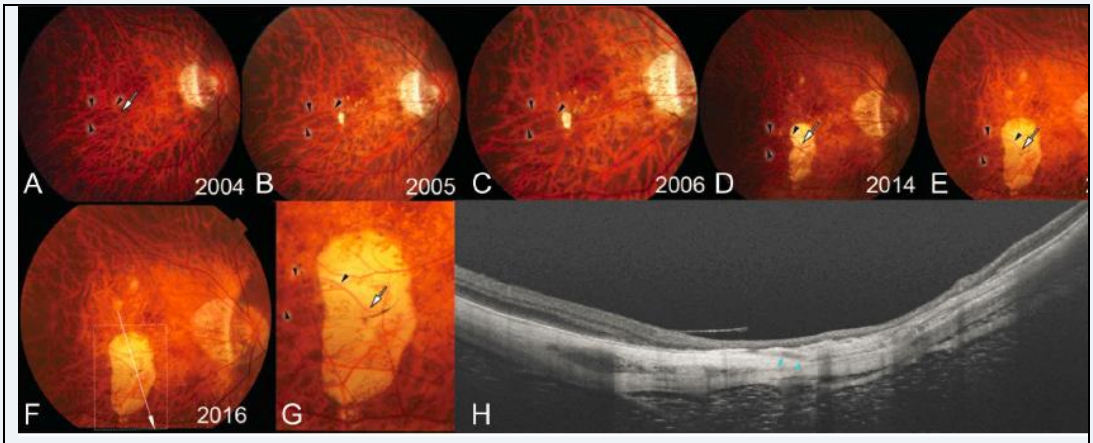

Fig. Long-term observation of PA that developed at the penetrating site of an AEV. A–E. Fundus photographs taken in 2004 to 2016, showing the formation and progression of PA originating from lacquer cracks. Black arrowheads in (A–E and G) indicate the same branches of the AEV. A. Fundus photograph taken in 2004. Tessellated fundus with no PA can be seen. The arrow shows a possible AEV penetrating site by comparing this photograph with the fundus in (D and E). B. A small PA has developed inferior to the fovea along lacquer cracks. Multiple lacquer cracks can be seen around the fovea. C–E. Further progression of the PA. Notice that the AEV is seen clearly within the PA area from the photograph taken in 2014 (arrow in D and E). F. Fundus photograph taken in 2016. The white arrow shows a scanned line by OCT in (H). G. Magnified image of the square area in (F). The white arrow indicates the AEV present within the PA. By comparisons of the vessel position, the PA probably developed at the AEV site. H. Optical coherence tomographic image shows the intrascleral course (blue arrowheads) of the perforating vessel that continuous to the AEV within the patchy atrophic area.

Abruptly emerging vessels are commonly found in eyes with myopic PA. The sclera surrounding the AEVs is slightly bowed. Further studies are needed to determine whether the penetrating site of AEVs is structurally more fragile and leads to Bruch membrane defects or AEVs are secondarily involved during PA progression.

In conclusion, AEVs were found in 43.1% of eyes with myopic PA. A slight bowing of the sclera was found around the AEVs in 41 of 69 eyes. Further clarification is needed on whether the penetrating site of AEVs makes the sites structurally fragile and cause macular BM defects or PA or the AEVs are secondarily involved in the enlargement of PAs.

Xie S et al. Retina. 2020 Jul;40(7):1215-1223. doi: 10.1097/IAE.0000000000002630.